Research Article | Vol. 24, No. 19 | 19 Sep 2016 | OPTICS EXPRESS 22232

Optics EXPRESS

Etalon filters for Brillouin microscopy of highly scattering tissues

PENG SHAO,[1] SEBASTIEN BESNER,[1] JITAO ZHANG,[2] GIULIANO SCARCELLI,[2] AND SEOK-HYUN YUN [1,3,*]

[1]*Wellman Center for Photomedcine, Massachusetts General Hospital and Havard Medical School, 50 Blossom Street, Boston, MA, 02114, USA*
[2]*Fischell Department of Bioengineering, University of Maryland, College Park, MD 20742, USA*
[3]*Harvard-MIT Health Sciences and Technology, Cambridge, MA 02139, USA*
[*]*syun@hms.harvard.edu*
https://www.intelon.org

Abstract: Brillouin imaging of turbid biological tissues requires an effective rejection of the background noise due to elastic scattering of probe laser light. We have developed a narrowband spectral notch filter based on a pair of a free-space Fabry-Perot etalon and a mirror. The etalon filter in a 4-pass configuration is able to suppress elastically-scattered laser light with a high extinction ratio of > 40 dB and transmit inelastically-scattered light in a frequency shift range of 2-14 GHz with only 2 dB insertion loss. We also describe a simple etalon that enables us to use semiconductor diode laser sources for Brillouin microscopy by removing spontaneous emission noise. Using a clinically-viable Brillouin microscope employing these filters, we demonstrate the first Brillouin confocal imaging of the sclera and conjunctiva of the porcine eye.

© 2016 Optical Society of America

OCIS codes: (300.6190) Spectrometers; (290.5830) Scattering, Brillouin.

References and links

1. G. Scarcelli, S. Besner, R. Pineda, and S. H. Yun, "Biomechanical characterization of keratoconus corneas ex vivo with Brillouin microscopy," Invest. Ophthalmol. Vis. Sci. **55**(7), 4490–4495 (2014).
2. F. Bencivenga, A. Battistoni, D. Fioretto, A. Gessini, J. R. Sandercock, and C. Masciovecchio, "A high resolution ultraviolet Brillouin scattering set-up," Rev. Sci. Instrum. **83**(10), 103102 (2012).
3. F. Palombo, M. Madami, D. Fioretto, J. Nallala, H. Barr, A. David, and N. Stone, "Chemico-mechanical imaging of Barrett's oesophagus," J. Biophotonics **9**(7), 694–700 (2016).
4. G. Scarcelli, P. Kim, and S. H. Yun, "In vivo measurement of age-related stiffening in the crystalline lens by Brillouin optical microscopy," Biophys. J. **101**(6), 1539–1545 (2011).
5. G. Scarcelli, P. Kim, and S. H. Yun, "In vivo measurement of age-related stiffening in the crystalline lens by Brillouin optical microscopy," Biophys. J. **101**(6), 1539–1545 (2011).
6. G. Scarcelli, W. J. Polacheck, H. T. Nia, K. Patel, A. J. Grodzinsky, R. D. Kamm, and S. H. Yun, "Noncontact three-dimensional mapping of intracellular hydromechanical properties by Brillouin microscopy," Nat. Methods **12**(12), 1132–1134 (2015).
7. G. Antonacci, G. Lepert, C. Paterson, and P. Török, "Elastic suppression in Brillouin imaging by destructive interference," Appl. Phys. Lett. **107**(6), 061102 (2015).
8. G. E. Devlin, "Absorption of unshifted scattered Light by a molecular I_2 filter in Brillouin and Raman Scattering," Appl. Phys. Lett. **19**(138), 138–141 (1971).
9. P. E. Schoen and D. A. Jackson, "The iodine filter in Raman and Brillouin spectroscopy," J. Phys. Educ. **5**(6), 519–521 (1972).
10. Z. Meng, A. J. Traverso, and V. V. Yakovlev, "Background clean-up in Brillouin microspectroscopy of scattering medium," Opt. Express **22**(5), 5410–5415 (2014).
11. A. J. Traverso, J. V. Thompson, Z. A. Steelman, Z. Meng, M. O. Scully, and V. V. Yakovlev, "Dual Raman-Brillouin microscope for chemical and mechanical characterization and imaging," Anal. Chem. **87**(15), 7519–7523 (2015).
12. A. Fiore, J. Zhang, P. Shao, S. H. Yun, and G. Scarcelli, "High-extinction virtually imaged phased array-based Brillouin spectroscopy of turbid biological media," Appl. Phys. Lett. **108**(20), 203701 (2016).
13. K. Berghaus, J. Zhang, S. H. Yun, and G. Scarcelli, "High-finesse sub-GHz-resolution spectrometer employing VIPA etalons of different dispersion," Opt. Lett. **40**(19), 4436–4439 (2015).
14. S. Besner, G. Scarcelli, R. Pineda, and S. H. Yun, "In vivo Brillouin analysis of the aging crystalline lens," Invest. Ophthalmol. Vis. Sci. (to be published).

#273034 http://dx.doi.org/10.1364/OE.24.022232
Journal © 2016 Received 3 Aug 2016; revised 31 Aug 2016; accepted 1 Sep 2016; published 15 Sep 2016

Optics EXPRESS

15. G. Scarcelli and S. H. Yun, "Multistage VIPA etalons for high-extinction parallel Brillouin spectroscopy," Opt. Express **19**(11), 10913–10922 (2011).
16. G. Scarcelli and S. H. Yun, "In vivo Brillouin optical microscopy of the human eye," Opt. Express **20**(8), 9197–9202 (2012).
17. B. Nemati, H. G. Rylander, and A. J. Welch, "Optical properties of conjunctiva, sclera, and the ciliary body and their consequences for transscleral cyclophotocoagulation," Appl. Opt. **35**(19), 3321–3327 (1996).
18. Y. Zhang, Z. Li, L. Liu, X. Han, X. Zhao, and G. Mu, "Comparison of riboflavin/ultraviolet-A cross-linking in porcine, rabbit, and human sclera," BioMed Res. Int. **2014**, 194204 (2014).
19. M. W. Ko, L. K. Leung, D. C. Lam, and C. K. Leung, "Characterization of corneal tangent modulus in vivo," Acta Ophthalmol. **91**(4), e263–e269 (2013).

1. Introduction

Brillouin microscopy allows for noninvasive, non-contact characterizations of materials by mapping hypersonic acoustic properties via light scattering spectroscopy [1]. For visible and near-infrared light, most materials generates spontaneous Brillouin frequency shifts in the order of 5-20 GHz. Traditionally, Brillouin spectrosacopy has been conducted by using tandem multi-pass Fabry Prot (FP) scanning interferometers [2, 3]. Improving data acquisition speeds, state-of-the-art Brillouin microscopes employ a single- or two-stage virtually imaged phased array (VIPA), and they have been applied to biomechanical characterizations of transparent corneas [4], crystalline lenses [5], and cells [6].

One of the general challenges in spontaneous Brillouin microscopy comes from low signal intensity given by the magnitude of natural thermodynamic fluctuations or acoustic phonons in the materials. The signal strength is typically several orders of magnitude lower than those of Rayleigh and Mie light scattering and Fresnel reflections from optical components in the path. Another challenge is the small frequency shift.

To differentiate Brillouin-shifted spectral components that are very close to the excitation laser line (<0.01 nm), conventional diffraction grating filters do not provide sufficient spectral resolution. The standard 2-stage VIPA spectrometer provides much higher resolution and a good extinction of about 60 dB. Although this extinction level is adequate for applications to translucent samples including the cornea and lens, but insufficient for turbid tissues, which generate strong elastic scattering that overshadows Brillouin scattering. A number of narrowband optical filters have been developed, which can be used in conjunction with a VIPA spectrometer to enhance extinction. Antonacci *et al*. [7] used a Michelson interferometer to suppress elastic scattering background with a rejection efficiency of 35 dB. However, free-space interferometry introduces mechanical instability and system complexity. Gas absorption cells have been used in Raman and Brillouin spectroscopy since the 1970s [8,9]. Recently Meng *et al.* [10] used Iodine vapor to filter out a 532-nm laser line in a two-stage-VIPA-based Brillouin microscope, obtaining a suppression of 50 dB, and Traverso *et al.* [11] used a Rubidium cell to filter a 780-nm laser line. However, gas absorption cells require specific wavelengths and heating to a temperature around 100 °C. Fiore *et al.* [12] used a triple-pass FP interferometer and obtained 30 dB, but the transmission band for Brillouin scattered light was narrow (<3 GHz).

In this paper, we report a new tunable etalon-based notch filter with advantages over previous filters in terms of high rejection (> 40 dB) for the narrowband laser line at a given frequency and low insertion loss (< 2 dB) for Brillouin signals over a broad frequency range (12 GHz). We also report the use of a laser clean-up etalon filter and wavelength locking to allow semiconductor lasers to be used as a light source, which typically have too high spontaneous-emission noise levels for Brillouin spectroscopy. Employing the two etalon filters in conjunction with a 2-stage VIPA spectrometer, we demonstrate Brillouin imaging of highly scattering ocular tissues in the sclera and the conjunctiva, which has previously not been possible with state-of-the-art Brillouin imaging systems.

Optics EXPRESS

2. Instrument design

Figure 1 (a) shows a schematic of the experimental setup. A single-frequency external-cavity diode laser with a wavelength tuning range around 780 nm (Vantage TLB-7113, New focus) was used as the light source. The output spectrum has a linewidth of 300 kHz and its center frequency can be tuned continuously by a voltage input. The typical wavelength drift of the laser output was measured to be as much as +/– 0.3 GHz over 5 min (+/– 1.2 GHz in 36 hr). The laser output beam is transmitted through a solid silica FP etalon that has a finesse of 7 and free-spectral range (FSR) of 16 GHz (LightMachinery Inc.). To lock the center frequency of laser emission to the transmission peak of the etalon, a small fraction (~4%) of the beam after the FP was tapped and measured with a photodetector. The voltage signal from the photodetector was used for active fine-tuning of the laser frequency to maintain a constant transmission through the etalon. An optical isolator (IO-5-780-VLP, Thorlabs) was placed to avoid unwanted feedback of optical reflection from the etalon. With this lock-in setup, the wavelength stability was improved to +/– 20 MHz, as measured with the 2-stage VIPA spectrometer, and the laser intensity after the clean-up etalon was stabilized to < 5%. The etalon acts as a cleanup filter to suppress the amplified spontaneous emission (ASE) background and spurious side-modes in the laser output. The magnitude of the ASE background light was measured to be –50 to –55 dB of the laser emission peak using a VIPA spectrometer. The broadband ASE background cannot be easily separated from Brillouin frequency-shifted signals once entering the VIPA etalons because they occupy the same physical space folded by the FSR of the VIPA [13]. The etalon cleanup filter [Fig. 1(b)] enabled us to effectively reduce the noise level to below –65 dB.

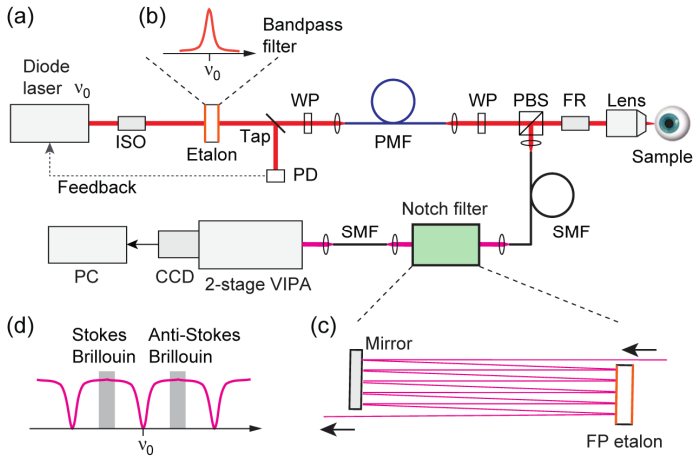

Fig. 1. (a) Schematic of the Brillouin microscope setup. ISO: optical isolator; WP: half-wavelength wave plate; PMF: polarization maintaining fiber; PD: photodetector; SMF: single mode fiber; PBS: 50/50 polarization beamsplitter; CCD: charge-coupled device camera, and PC: personal computer; FR: Faraday Rotator. (b) Illustration of a transmission band of the cleanup etalon. The laser output frequency, ν_0, is tuned and locked to the center frequency of the passband. (c) A schematic of the notch filter made with an etalon paired with a mirror for multiple, frequency-selective reflections by the etalon. (d) Illustration of the transmission spectrum of the notch filter. The signal ranges for frequency-shifted Brillouin light are marked with gray.

The laser beam after the cleanup filter was delivered to a sample through a single-mode polarization-maintaining optical fiber (PMF) and an objective lens (20 × , NA = 0.42, Mitutoyo). The scattered light from the sample was collected by the lens and directed to a receiving single mode fiber (SMF) via a non-reciprocal Faraday rotator (I-80-4-FR, Isowave) and a polarization beam splitter. After the SMF, we placed the notch filter we have developed to remove elastically scattered light and transmit Brillouin scattered light.

Optics EXPRESS

Figure 1(c) depicts the notch filter based on a solid FP etalon with an FSR of 16 GHz (thickness ~6.4 mm) and low finesse of ~7. The etalon's FSR was matched to that of the VIPA spectrometer, and the relatively low finesse was chosen to optimize high extinction, low loss, and ease of implementation. Higher finesses might be used, but they would require increasingly challenging beam alignments and cause higher sensitivity to mechanical and temperature drifts. The etalon was made of fused silica with relatively low temperature-dependent refractive index. The etalon is tilted with respect to the entrance beam path at such an angle that the laser frequency is resonant with the etalon and transmits with maximum loss, whereas the rest of the spectrum including Brillouin signals is reflected. A silver-coated mirror allows the input beam to undergo multiple reflections from the etalon. On each reflection, the remaining light at the laser frequency is mostly transmitted through the etalon and thereby further filtered out.

The output of the notch filter is transmitted via a single-mode fiber (SMF) to a custom-built spectrometer. The SMF is not essential, and the output of the filter may be arranged to enter the spectrometer directly. The spectrometer consists of two-stage VIPA etalons and an electron multiplying charged coupled device camera (EMCCD, iXon U897, Andor Technology), connected to a computer for data processing and display [14].

3. Experimental results

To optimize the notch filter, we measured the rejection efficiency and insertion loss of the device as a function of the number of reflections from the etalon, which we varied by changing the tilt angle of the etalon and mirror. The results are plotted in Fig. 2. The extinction in the logarithmic scale is enhanced with the number of reflections at a slope of ~10 dB per reflection, reached at 40 dB with a 4-reflection design. Beyond five reflections, the rejection saturated presumably due to stray light and finite flatnesses of the etalon and mirror. The transmission decreases linearly with the number of reflections and was ~66% (~1.8 dB loss) with the 4-pass configuration.

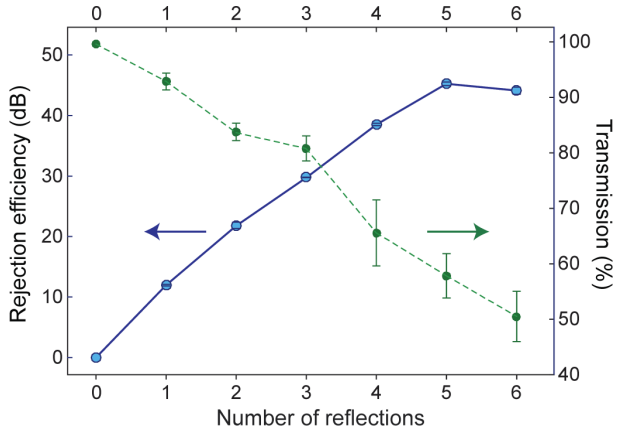

Fig. 2. The spectral extinction (left axis) and throughput (right axis) efficiencies measured as a function of the number of reflection passes in the notch filter.

We then measured the extinction of the laser output through the entire Brillouin microscope system by placing a mirror at the sample plane and attenuating the reflected light. Figure 3 shows the spectrographs recorded in the CCD of the VIPA spectrometer before and after employing the notch filter in the detection path (Fig. 1). A suppression of ~40 dB at the laser line was achieved by a 4-reflection notch filter. The overall noise floor in the signal frequency bands was at about –65 dB and not lowered by the filter. This is because the noise floor at –65 dB was given by the spontaneous emission light in the laser spectrum, which is not removed by the notch filter. In principle, the laser noise level can be improved by using

Optics EXPRESS

clean-up etalons with higher extinction. We note that in actual Brillouin imaging of turbid samples, the detection noise is often limited by the stray light of the laser light within the spectrometer; therefore, the ability to attenuate the laser line before it enters the VIPA spectrometer, without inducing loss to other frequency components, is essential for turbid tissue imaging, as we demonstrate next.

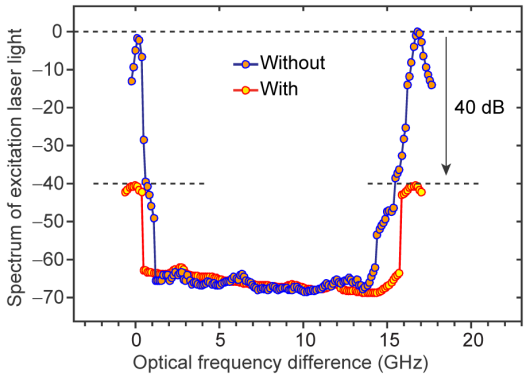

Fig. 3. The spectra of the laser output recorded in a 2-stage VIPA spectrometer without (blue circles) and with (orange circles) a 4-pass etalon notch filter with a FSR of 16 GHz. The extinction at the locations (0 and 16 GHz) corresponding to the laser frequency is improved by 40 dB by the filter. The noise floor at –65 dB is due to the spontaneous emission light in the laser output, which is invariant by the narrowband filter rejecting the laser line.

To test the Brillouin system with turbid samples, we first used Intralipid (lipid emulsion, Sigma-Aldrich Corp.) solutions with various concentrations from 0% (pure distilled water) to 10%. Standard transparent macro disposable cuvette (BRAND, Sigma-Aldrich Corp.) was used as the solution container during imaging. Figure 4 depicts the Brillouin signal counts and background fluctuation noise recorded with the 4-pass notch filter and VIPA spectrometer. Without the notch filter, the standard 2-stage VIPA spectrometer alone cannot clearly discern Brillouin peaks from the background noise even at a low Intralipid contraction of 0.001%, and the signal-to-noise ratios are below 1 (i.e. nonmeasurable) at concentrations higher than 0.01% [15].

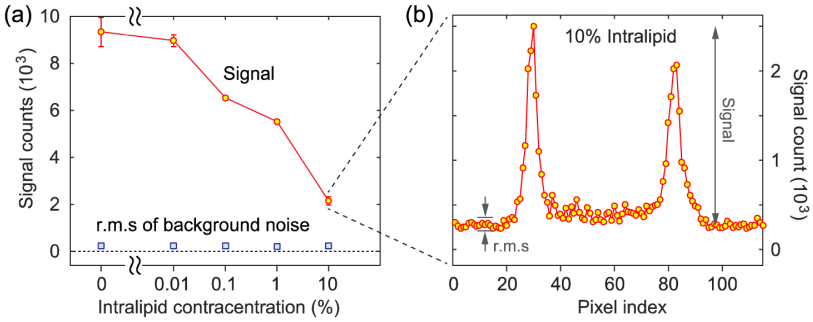

Fig. 4. Brillouin measurements of lipid emulsion solutions. (a) The magnitude of signal and r.m.s. fluctuation of the background noise. (b) A representative spectral curve obtained with Intralipid 10%. The data were averaged over 5 spectrographs acquired with an integration time of 1 s each.

Next we tested the Brillouin system with highly scattering biological tissues. Figure 5 shows representative EMCCD recordings obtained from a piece of porcine conjunctiva tissue without and with the norch filter. In the CCD plane of the two-stage spectrometer, the central, horizontal line represent the spectral signal axis, whereas noise and stray light occupies the entire area [15]. The signal strengths along the horizontal lines are nearly unchanged by the

Optics EXPRESS

notch filter, but the dramatic reduction of the noise in the entire CCD plane by filtering is apparent. The excessive background noise without the additional notch filter has limited previous VIPA-based Brillouin systems to transpatent tissues, such as the cornea and crystalline lens [16].

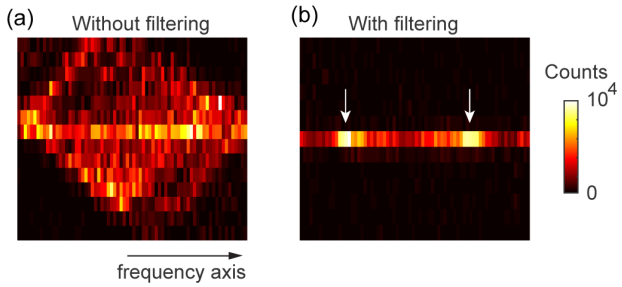

Fig. 5. Representative EMCCD readings for scatterd light from the porcine conjunctiva, obtained without, (a), and with, (b), the notch filter. The background noise in (a) is greatly reduced in (b) where the Stokes and anti-Stokes Brillouin peaks (arrows) are clearly seen.

Using the improved setup, we performed Brillouin imaging of fresh porcine eyeballs within 12 hours *post mortem*. Figure 6 shows representative 2D Brillouin frequency-shift maps of the cornea, conjunctiva, and sclera. The corneal and scleral images depict depth-averaged mean Brillouin frequency shifts at 10-20 locations below the tissue surface. The image of limbal conjunctive was obtained from a depth range of 100 to 200 μm below the epithelium. The laser power was 5 mW on the sample surface. The light scattering coefficients of the conjunctiva are known to be similar to those of chicken breast tissues, and the light scattering from the sclera is about 10 times stronger than the scattering from the conjunctiva [17]. Different camera integration times of 1, 2, and 4 s were used for the cornea, conjunctiva, and sclera, respectively, to compensate for the reduced signal strength proportional to the amount of light scattering. The conjunctiva tissues showed significantly higher Brillouin shifts than the cornea, and the sclera exhibited much higher Brillouin shifts. The typical ranges of the reported Young's moduli of porcine tissues are ~1-4 MPa of scleral tissues [18], much higher than ~0.1-0.5 MPa for corneas [19] (We were unable to find Young's modulus of conjunctiva tissues in literature). The individual data in the Brillouin maps are plotted in Fig. 7. The difference of Brillouin shifts between tissue types is statistically significant (p-values < 0.001)

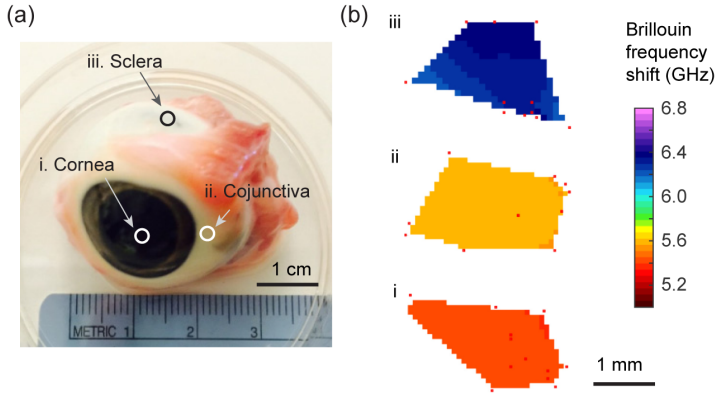

Fig. 6. Brillouin imaging of scattering tissues. (a) Porcine eye ball sample. The scanned areas (i-iii) are marked. (b) 2D Brillouin frequency shift maps of the (i) cornea, (ii) conjunctiva and (iii) sclera from the eyeball sample. The red dots indicate individual locations, each of which a Brillouin axial profile was acquired and depth-averaged mean frequency shift was computed.

Optics EXPRESS

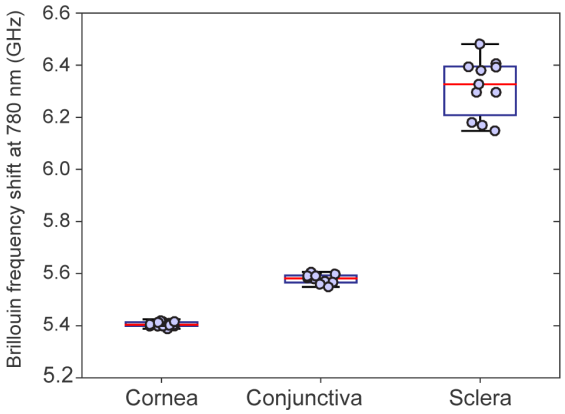

Fig. 7. Brillouin frequency-shift values of three representative tissue types in the porcine eye (as indicated in Fig. 6), measured at a laser wavelength of 780 nm.

4. Conclusion and discussion

The FP-based narrowband notch filter we have constructed with a single etalon in multi-pass reflection mode provided a high background rejection rate of > 40 dB with a low insertion loss of < 2 dB. This approach dose not require heating as gas cell filters, or mechanical movement as interferometer filters, and therefore does not introduce system complexity. When employed in a clinically-viable Brillouin imaging system, this filter enabled us to obtain Brillouin data from the conjunctiva and sclera, for the first time to our knowledge. For imaging the transparent cornea or crystalline lens, the notch filter may allow us to use a single-stage VIPA spectrometer with an advantage of simplicity and low insertion loss (3-5 dB loss in the second stage).

We also described a spectral cleaning scheme based on an etalon in the transmission mode, which enabled us to use a semiconductor laser light source for Brillouin imaging. The frequency locking to the etalon provided improved long-term stability of the system. The current system in a temperature-regulated lab environment showed a small drift in Brillouin signal strength of about ± 1 dB over 1 h. If necessary, all spectral elements including the notch filter and VIPA etalons could be locked to the laser frequency.

Funding

National Institutes of Health (R01EY025454, K25EB015885, R33CA204582); National Science Foundation (CBET-562863, CMMI-1537027); Harvard Catalyst Incubator program (UL1-RR025758); MGH Research Scholar award program; Human Frontier Science Program (RGY0074); Natural Sciences and Engineering Research Council of Canada (NSERC) post-doctoral fellowship (to P.S.).

Acknowledgments

We thank Sun-Joo Jang, Niaz Karim, Lawrence Yoo, Dominik Beck, and Theo Seiler Jr. for helpful comments.

132.183.13.50 {ts '2016-10-05 11:34:48'}